Anal Bioanal Chem
DOI 10.1007/s00216-007-1382-0

ORIGINAL PAPER

Spectral elucidation of the acid metabolites of the four geometric isomers of trifloxystrobin

Kaushik Banerjee · Axel Patrick Ligon · Michael Spiteller

Received: 23 February 2007 / Revised: 10 May 2007 / Accepted: 22 May 2007

Abstract Four geometric isomers of trifloxystrobin (TFS)—namely *EE*, *EZ*, *ZE*, and *ZZ*—were hydrolyzed by 0.05 M NaOH, resulting in four corresponding acid metabolites. These compounds—namely *EE*-, *EZ*-, *ZE*-, and *ZZ*-acids—were purified by preparative HPLC and authentically characterized by a combination of infrared, Raman, GC–MS, LC–MS/MS, and NMR spectroscopies. The spectra were found to be very characteristic of the individual isomers, and so they could be used to distinguish the isomers from each other. The detailed spectral features of the individual isomers are presented and compared. *EE*-acid was identified as being the major metabolite of TFS in soil, which indicates that hydrolysis is the principal route of degradation of TFS. This finding further justifies the importance of the present study in relation to assessing the risk associated with the release of TFS into the environment.

Keywords Trifloxystrobin · Hydrolysis · HPLC · IR · Raman · NMR · Mass spectroscopy

Introduction

Trifloxystrobin [methyl-α-(methoxyimino)-2-[({1-[3-(trifluoromethyl)-phenyl]ethylidene}amino)oxymethyl]benzeneacetate] is a systemic fungicide developed by Novartis and marketed by Bayer Crop Science [1]. It is the first strobilurin compound with an oximether side chain, which exhibits broad-spectrum fungicidal bioefficacy against a variety of crop pests [2, 3]. We have reported the photoisomerization kinetics of TFS [4] and shown how it gets converted to four geometrical isomers—namely *EE*, *EZ*, *ZE*, and *ZZ*—upon exposure to sunlight. We isolated all four isomers in pure crystalline form and reported the X-ray crystallographic structures of the *ZZ*, *ZE*, and *EZ* isomers [5–7], which do not exhibit biological activity against target microorganisms. Since TFS and its isomers are esters by nature, they are susceptible to hydrolysis, resulting in the formation of the corresponding acid metabolites. We were able to produce the monocarboxylic acid metabolite of TFS (*EE*-acid) by alkaline hydrolysis under in vitro conditions and we reported its X-ray crystallographic structure [8]. The *EE*-acid does not present any bioefficacy against target pests like *Botrytis cinerea* [9, 10]. However, it was identified as the major metabolite of TFS in soils [11]. Similarly, the other three isomers of TFS, once they enter the environment, can also get hydrolyzed to the corresponding acid metabolites. Since they are more water-soluble than their parent esters, these compounds have more potential to contaminate the environment and cause harm to beneficial flora and fauna. Hence, it is essential to characterize these hydrolysis products from TFS so that a holistic risk assessment of the release of TFS into the environment can be performed and suitable strategies for their remediation can be developed. In the present work, we attempted to characterize the four acid metabolites of TFS isomers by a combination of infrared (IR), Raman, NMR-, and mass spectrometries, which are all considered to be very powerful tools for distinguishing such isomers from each other.

K. Banerjee
National Research Centre for Grapes,
Pune 412 307, India

A. P. Ligon · M. Spiteller (✉)
Institute of Environmental Research (INFU),
University of Dortmund,
Otto-Hahn-Strasse 6,
44221 Dortmund, Germany
e-mail: m.spiteller@infu.uni-dortmund.de

Materials and methods

Materials

Reference standards of the TFS isomers were obtained from Bayer Crop Science (Monheim, Germany). All reagents and solvents used for the chromatographic, spectroscopic, and photolytic procedures were of analytical quality or higher. The water used in the mobile phase for HPLC was purified by means of a Milli-Q-Plus 185 system (Millipore Corporation, Bedford, MA, USA).

Chromatographic methods

HPLC

Chromatographic purification of the TFS isomers and the individual acid metabolites was performed with a Gynkotek (Germering, Germany) HPLC equipped with a preparative Kromasil 100 C18 column (250×20 mm, 7 μm; Eka Chemicals, Bohus, Sweden) and a UV detector set at 250 nm. The mobile phase was acetonitrile:water (90:10, v/v) at a flow rate of 4 mL/min.

The analytical HPLC was performed on a Phenomenex (Torrance, CA, USA) RP-18 column (150 mm×2 mm, 3 μm) under the same chromatographic conditions as above, except for a flow rate of 0.2 mL/min.

IR/Raman

IR spectra were recorded in KBr pellets on a Bruker Analytik (Karlsruhe, Germany) IFS 28 FTIR spectrometer with a Globar source, a Ge/KBr beam splitter and a DTGS detector. Atmospheric water vapor and carbon dioxide were removed from the measuring chamber with the help of dry nitrogen gas. All spectra were recorded at a resolution of 2.0 cm^{-1} and 100 scans were made.

The Raman spectra were acquired on Horiba Jobin-Yvon Inc. (Edison, NJ, USA) 60000 triple monochromator spectrometer equipped with a Spectra-Physics (Mountain View, CA, USA) model 164 argon ion laser operated on the 514.5 nm line. The laser power used was 100 mW, with a spectral band-space of 3 cm^{-1}. The Raman spectra of the solid crystal powders were measured in a glass capillary.

Mass spectrometry

GC–MS

GC–MS analyses were performed with Thermo Finnigan (San Jose, CA, USA) Trace GC equipment, equipped with a Trace MS^{PLUS} detector, operated in full-scan mode (40–450 amu) at an ionization energy of 70 eV. The gas chromatograph was operated in split/splitless injection mode with the injector at a temperature of 280 °C and a split flow of 50 mL/min; the injection volume was 1 μL. The compounds were separated on a DB 5 column (30 m× 0.25 mm, 0.25 μm). Helium was used as carrier gas at a flow rate of 1.1 mL/min, and the column temperature was programmed from 50 to 300 °C at 15 °C/min.

HPLC–MS–MS

Analysis was performed with Thermoquest TSQ 7000 Finnigan triple quadrupole mass spectrometer hyphenated to the Gynkotek HPLC. Atmospheric pressure chemical ionization (APCI) was performed in positive-ion mode; the corona discharge current was 4 A, the capillary temperature 180 °C, and the ion source temperature was set to 450 °C.

Nuclear magnetic resonance (NMR) spectroscopy

NMR spectroscopy was performed with a Varian (Palo Alto, CA, USA) Inova 600, a 600 MHz instrument, with anhydrous DMSO-D_6 used as solvent. The concentration of each isomer in solution was 1 mg/mL. The NMR spectra were recorded in both one-dimensional (1-D) and two-dimensional (2-D) modes. The 1-D mode involved recording ^{1}H and ^{13}C APT spectra. 2-D NMR techniques included correlation spectroscopy (gCOSY), heteronuclear multi-bond correlation (gHMBC), and heteronuclear single quantum coherence (gHSQC). gCOSY was performed to investigate the coupling of two protons. gHMBC reflects long-range CH correlation over two or three bonds, whereas gHSQC establishes direct CH correlation.

Photoisomerization of TFS

Source of light

A Suntest apparatus (Heraeus, Hanau, Germany) was used to irradiate the TFS in solution. This system contains a xenon lamp with an irradiation spectrum similar to that of sunlight. The intensity of the radiation is adjustable over the range 150–800 W/m^2.

Irradiation of TFS

Irradiation was conducted in pure acetone medium in a quartz vessel. Acetone was selected since TFS is highly soluble in acetone; it works as an excellent photosensitizer, and is also easy to handle. Nonradioactive TFS (>99% pure, 200 mg) was accurately weighed into the quartz vessel. TFS was completely dissolved in 50 mL solvent at room temperature, upon gentle shaking. The quartz vessel was placed inside the Suntest apparatus and irradiated at

500 W/m^2. The reaction solutions were sampled at regular time intervals to monitor the formation of the photoisomers by analytical HPLC until an equilibrium mixture of the four isomers was achieved.

Isolation and identification of the TFS isomers

The four isomers of TFS were separated by reversed-phase preparative HPLC, as described earlier [4]. The pure isomeric compounds thus obtained were crystallized from methanol at room temperature. The identities of the isomers were further confirmed through comparison with the reference standards by HPLC–MS/MS.

Preparation of acid metabolites

The acid metabolites corresponding to the four individual isomers of TFS were produced by alkaline hydrolysis of the individual isomers separately with 0.05 M NaOH in a medium of acetone:0.05 M NaOH in water (50:50 v/v) at 293 K performed under continuous stirring achieved using a magnetic stirrer. The completion of the hydrolysis was monitored by HPLC. Once all of the parent compound was hydrolyzed, the reaction mixture was neutralized with 0.05 M HCl and evaporated at <40 °C. The residue was redissolved in acetonitrile and further purified by preparative HPLC. All four acid metabolites separated out as white solids from the corresponding combined eluate.

Monitoring the residue dynamics of the acid metabolites in a soil environment

The residues of the four acid metabolites were investigated in a silty clay soil of USDA class of Typic Ustochrepts. TFS was mixed with the soil at the recommended commercial use rate of 500 g active ingredient ha^{-1}. The experimental design used was based on the EC Directive [12], the SETAC procedures [13], the BBA guideline [14], and the FDA technical assistance handbook [15]. Batches of 100 g soil (relative to dry soil) were incubated in Erlenmeyer flasks at controlled temperature (20±1° C) in darkness. The moisture content of the test soil was adjusted to 60% of its maximum water holding capacity and gravimetrically checked once in every two weeks. The samples were drawn on 0, 1, 3, 7, 14, 31, and 90 days after application. All of the soil samples were analyzed for the residues of TFS, its *EZ*, *ZE*, and *ZZ* isomers, and the four acid metabolites by LC–MS/MS [11].

Results and discussion

The four geometric isomers of TFS eluted with good baseline separation at retention times (RT) of 16.9, 18.2, 19.3, and 20.9 min when analyzed by HPLC. By comparison with the reference standards, they were identified as the *EZ*, *EE*, *ZZ*, and *ZE* isomers, respectively. The isomerization process reached equilibrium after approximately 7 h of illumination, as described earlier [4], when the *EZ*/*EE*/*ZZ*/*ZE* ratio was 2.8:2.2:1.4:1. No degradation of TFS to inorganic molecules (mineralization) was observed during illumination. The alkaline hydrolysis of the above equilibrium mixture of isomers with 0.05 M NaOH resulted in four additional peaks in HPLC, separated at RTs of 13.6, 14.7, 15.0, and 16.5 minutes. Upon LC–MS analyses, all these hydrolysis products were found to have the same protonated mass of *m/z* 395 and it was therefore concluded that they were monocarboxylic acid metabolites of the four isomers of TFS. This observation was further confirmed by performing comparative LC–MS/MS analyses of TFS isomers and their acid metabolites, whereupon we observed the appearance of a peak at *m/z* 192 (see structure in Table 4) at a collision energy of −15 eV in place of that at *m/z* 206 (*m/z* 192 − H + CH_3) observed for the parent esters [4]. The EE-acid was unambiguously identified upon comparison with the pure reference standard produced by us. The other three acid metabolites were tentatively identified as the *EZ*-acid, the *ZZ*-acid, and the *ZE*-acid, depending on their relative retention times.

Table 1 Vibrational data (cm^{-1}) and assignments of the *EE*-, *EZ*-, *ZE*-, and *ZZ*-acids

ZE		*ZZ*		*EE*		*EZ*		Assignment
IR	Raman (solid)	IR	Raman (solid)	IR	Raman (solid)	IR	Raman (solid)	
1707 1721	1672 (weak)	1743	–	1705	1706 1710	1701	1709	ν(C=O)
1617 (weak)	1623	1608 (weak)	1625	1619 (weak)	1625	–	1625	ν(C=N)
1588 (weak)	1608 1593	1609	1604	–	1596	1605 1603	1610 1596	ν(8a)
–	1577	1589	1567	1586	1579	1581	1578	ν(8a)

Table 2 EI-mass spectroscopic data of four acid metabolites

Fragment	Structure	m/z	Intensity			
			EZ	ZZ	EE	ZE
$[M]^{+\cdot}$		394	-	-	-	-
$[M - H_3]^{+\cdot}$		391	1.07	8.02	1.02	5.80
$[C_{11}H_{12}N_2O_4]^{+\cdot}$	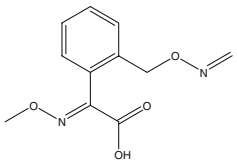	236	8.30	39.12	13.54	45.16
$[C_{11}H_{12}N_2O_3]^{+\cdot}$	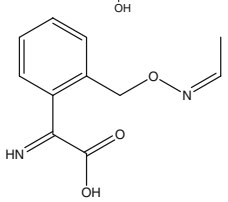	220	17.81	81.45	10.40	51.09
$[C_{10}H_{10}NO_3]^{+\cdot}$	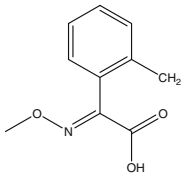	192	1.16	60.79	1.26	49.99
$[C_{10}H_8NO_3]^{+\cdot}$		190	4.07	33.36	6.49	36.68
$[C_9H_7NF_3]^{+\cdot}$	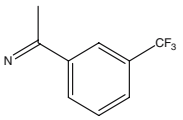	186	10.07	59.43	11.15	60.09
$[C_9H_8NO_2]^{+\cdot}$	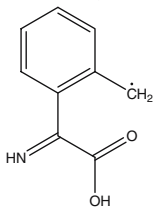	162	1.35	28.80	1.75	30.28
$[C_7H_4F_3]^{+\cdot}$	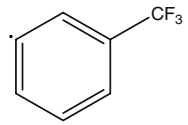	145	8.87	26.00	11.33	33.25
$[C_{10}H_9N]^{+\cdot}$		143	0.97	13.75	0.51	11.68
$[C_8H_6NO]^{+\cdot}$	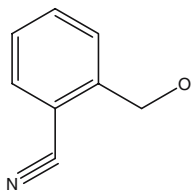	132	7.89	99.01	9.60	100
$[C_8H_6N]^{+\cdot}$	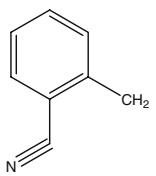	116	100	100	100	93.74
$[C_7H_6N]^{+\cdot}$		104	2.75	15.98	2.62	14.25
$[C_7H_5]^{+\cdot}$		89	7.32	22.84	7.51	19.98
$[C_6H_5]^{+\cdot}$		77	3.85	22.49	3.74	18.72

Table 3 Intensities (%) of the product ions from the *EE*-acid precursor ion *m/z* 395 at different collision energies

Colisional energy (eV)	*m/z* 395	*m/z* 192	*m/z* 186	*m/z* 148	*m/z* 145	*m/z* 116
−15	100.0	14.9	86.4	15.7	0.0	0.0
−20	4.1	10.2	100.0	39.1	0.0	6.6
−25	0.0	4.6	100.0	33.6	1.5	13.8
−30	0.0	3.7	100.0	22.9	11.1	21.9
−35	0.0	3.5	100.0	17.4	24.1	35.0
−40	0.0	1.3	100.0	11.8	44.1	39.4

Separate alkaline hydrolyses of the individual *EZ*, *ZZ*, and *ZE* isomers of TFS with 0.05 M NaOH and subsequent LC–MS/MS analysis further confirmed the identities of these three acid metabolites.

The vibrational spectral assignment for the four acids is presented in Table 1. The lack of conjugation of the toxophore group with the ortho-substituted aromatic ring may be the reason for the normal value of the ν(C=O) group in the *EE*- and *ZE*-acids in both the IR and the Raman spectra. In the *EZ*-acid, a strong band was observed for ν(C=O) in IR, which became weak in the Raman spectrum. In the *ZZ*-acid, the band for ν(C=O) was absent in the Raman spectra. The signal for ν(C=N) in the IR spectra of the *EE*- and *ZE*-acids was weak and absent in the *EZ*-acid. In the Raman spectra of the *ZE*- and *ZZ*-acids, strong and medium signals, respectively, were observed for ν(C=N), whereas in the *EE*- and *ZZ*-acids, ν(C=N) was very weak. In the *ZZ*-acid, the *Z*-system in the methoxy part connected to the *o*-substituted aromatic system may build a ring structure through hydrogen bonding between the oxime ether and ester moieties. Further, the *Z*-system between the aromatic rings is under pressure/stress in the *ZZ*-acid. As the CO in the *ZZ*-acid is sterically hindered, the ν(C=O) may shift to a higher wavenumber. This assignment is in agreement with the results of Kaczor et al., [16] who found the ν(C=N) at 1648 cm^{-1} in the IR spectrum, and this result was confirmed by DFT and MP2 calculations. The extremely high intensity of the ν(C=N) bands for the ZZ isomer could be explained by so-called "intensity borrowing" of ν(C=N) from the ν(8a) band. The same phenomenon is described in the literature [17], but it is yet to be fully explained. We suggest that this

Table 4 MS/MS spectroscopic data for four acid metabolites from the precursor ion *m/z* 395 at the collision energy of −20 eV

Fragment	Structure	m/z	Intensity			
			EZ	ZZ	EE	ZE
$[M+H]^+$		395	4.1	0.0	4.1	1.2
$[C_{10}H_{10}NO_3]^{+\cdot}$	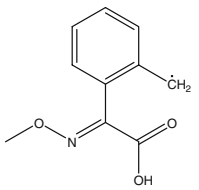	192	14.1	20.6	10.1	17.1
$[C_9H_7NF_3]^{+\cdot}$	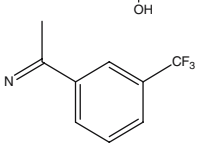	186	36.2	18.2	100.0	100.0
$[C_9H_{10}NO]^{+\cdot}$	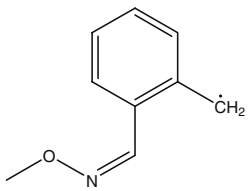	148	100.0	100.0	39.1	39.7
$[C_8H_6N]^{+\cdot}$	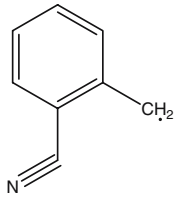	116	8.2	7.9	6.6	7.1

Table 5 ^{1}H NMR signals for the four acid metabolites; coupling constants in Hz

Carbon (C) number	*EE*-acid [δH (ppm)]	*ZE*-acid [δH (ppm)]	*EZ*-acid [δH (ppm)]	*ZZ*-acid [δH (ppm)]
1	–	–	–	–
2	–	–	–	–
3	3.89 *s*	3.93 *s*	3.87 *s*	3.71 *s*
4	–	–	–	–
5	7.18 *dd* ($^{3}J_{5,6}$=6,60) ($^{4}J_{5,7}$=0,92)	7.40 *dd* ($^{3}J_{5,6}$=7,69) ($^{4}J_{5,7}$=1,10)	7.15 *d* ($^{3}J_{5,6}$=8,42)	7.50 *d* ($^{3}J_{5,6}$=7,33)
6	7.38 *dt* ($^{3}J_{6,5;6,7}$=7,83) ($^{4}J_{6,8}$=1,10)	7.43 *dt* ($^{3}J_{6,5;6,7}$=7,51) ($^{4}J_{6,8}$=0,73)	7.35 *m* (*J*=6,96)	7.24 *m*
7	7.41 *dt* ($^{3}J_{7,6;7,8}$=7,70) ($^{4}J_{7,5}$=1,23)	7.50 *dt* ($^{3}J_{7,6;7,8}$=6,96) ($^{4}J_{7,5}$=1,47)	7.38 *t* ($^{3}J_{7,6;7,8}$=7,69)	7.26 *m*
8	7.47 *d* ($^{3}J_{8,7}$=7,33)	7.57 *d* ($^{3}J_{8,7}$=7,69)	7.35 *d* ($^{3}J_{8,7}$=6,23)	7.27 *m*
9	–	–	–	–
10	5.07 *s*	5.44 *s*	4.85 *s*	5.30 *s*
11	–	–	–	–
12	2.21 *s*	2.33 *s*	2.16 *s*	2.21 *s*
13	–	–	–	–
14	7.91 *d* ($^{3}J_{14,15}$=8,06)	7.96 *d* ($^{3}J_{14,15}$=8,06)	7.78 *d* ($^{3}J_{14,15}$=7,69)	7.92 *d* ($^{3}J_{14,15}$=7,69)
15	7.64 *t* ($^{3}J_{15,14;15,16}$=7,87)	7.64 *t* ($^{3}J_{15,14;15,16}$=7,87)	7.65 *t* ($^{3}J_{15,14;15,16}$=8,06)	7.69 *t* ($^{3}J_{15,14;15,16}$=7,88)
16	7.76 *d* ($^{3}J_{16,15}$=7,69)	7.77 *d* ($^{3}J_{16,15}$=7,69)	7.74 *d* ($^{3}J_{16,15}$=7,69)	7.76 *d* ($^{3}J_{16,15}$=7,69)
17	–	–	–	–
18	7.90 *s*	7.94 *s*	7.85 *s*	7.97 *s*
19	–	–	–	–

Table 6 ^{13}C NMR signals for the four acid metabolites

Carbon (C) number	*EE*-acid [δC (ppm)]	*ZE*-acid [δC (ppm)]	*EZ*-acid [δC (ppm)]	*ZZ*-acid [δC (ppm)]
1	163.64	164.08	163.59	165.69
2	149.82	151.60	149.53	159.13
3	62.85	62.39	62.82	60.75
4	130.68	128.32	130.16	131.62
5	128.44	128.51	128.26	128.89
6	127.53	127.79	127.30	126.69
7	128.69	129.76	128.71	127.88
8	128.47	128.57	128.09	126.60
9	135.33	136.95	135.37	136.58
10	74.30	73.45	73.21	73.44
11	153.53	153.91	152.54	152.34
12	12.18	12.48	20.86	20.93
13	136.73	136.76	137.73	135.01
14	129.84	129.91	131.89	132.06
15	129.56	129.62	129.13	129.39
16	125.61	125.71	125.47	125.57
17	124.70	124.87	123.16	123.16
18	122.08	122.12	124.29	124.58
19	123.06	123.04	121.40	121.36

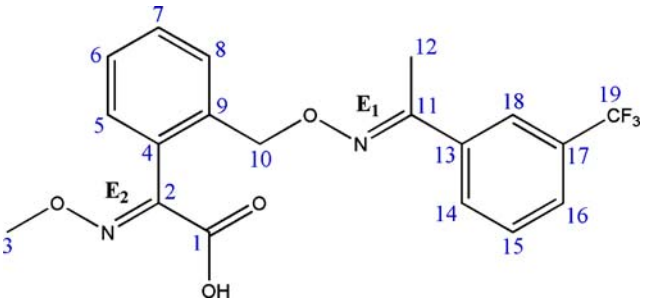

Fig. 1 The geometric structure of trifloxystrobin acid (*EE* isomer)

phenomenon requires deep and systematic explorations supported by suitable isotopic labeling.

All of the isomeric acids may have C_1 symmetry, as suggested by the simultaneous IR and Raman activities of all normal modes. The region around 1600 cm^{-1} is quite interesting because the C=N stretching and the two-ring stretching (vibrational pair 8a according to Wilson nomenclature) absorb here [18]. In the Raman spectra of all of the isomers, the bands between 1611 and 1567 cm^{-1} are strong or very strong, and these bands are assigned to 8a, in agreement with literature data [19–23].

The EI–MS data for the four isomers along with the probable structures of the fragment ions are presented in Table 2. Nine major fragments were identified. The molecular ion could not be identified in any of the spectra. Comparison of the mass spectra shows that the double bond N=C connected to the meta-substituted benzene ring controls the type of the base peak. The mass spectra for the *EE*-acid and the *EZ*-acid were similar, and this similarity was also observed between the *ZZ*-acid and the *ZE*-acid. The base peaks of the *EE*-, *EZ*-, and *ZZ*-acids were the same (*m/z* 116), which is also the same as the base peak observed for their corresponding parent ester, as reported earlier [4]. On the other hand, the base peak for the *ZE*-acid was observed at *m/z* 132, which is also different from the base peak of its parent *ZE*-ester, observed at *m/z* 206 [4]. In the *ZZ*-acid we also observed the peak at *m/z* 132 with >99% intensity, but the intensity of this *m/z* is <10% in the *EE*- and *EZ*-acids. The stability of *m/z* 220 was quite significant in the *ZZ*-acid, indicating the formation of a ring structure between the oxime ether and the ester moiety connected to the ortho-substituted aromatic system. The intensity of *m/z* 220 was, however, much less in the *ZE*-acid and also <20% for the *EE* and *EZ* conformations. Similarly, the intensities of *m/z* 192 and 190 in *ZZ* and *ZE* were significant, but these were <2% in the *EE*- and *EZ*-acids.

The full-scan LC-MS spectra of all of the isomers showed that a protonated molecular ion gave rise to the base peak at *m/z* 395. The developments of different fragment ions and their intensities for the *EE*-acid at different collisional energies (−eV) are presented in Table 3. The fragment ions of the four acids were compared at a collisional energy of –20 eV and are presented in Table 4 along with their most probable structures. The most stable fragment was the same for the *EE*- and *EZ*-acid pair and for the *ZE*- and *ZZ*-acid pair. In the *EE* and *ZE* conformations, the C=N bond in the acid part is in the *E* orientation, which gets fragmented upon collision with the inert gas in MS/MS during the pathway *m/z* 395→186. At *m/z* 186, the vibration energy of the molecule might get stabilized enough to form a stable daughter ion for the *EE*- and *ZE*-acids. In the *EZ* and *ZZ* conformations, the fragmentation

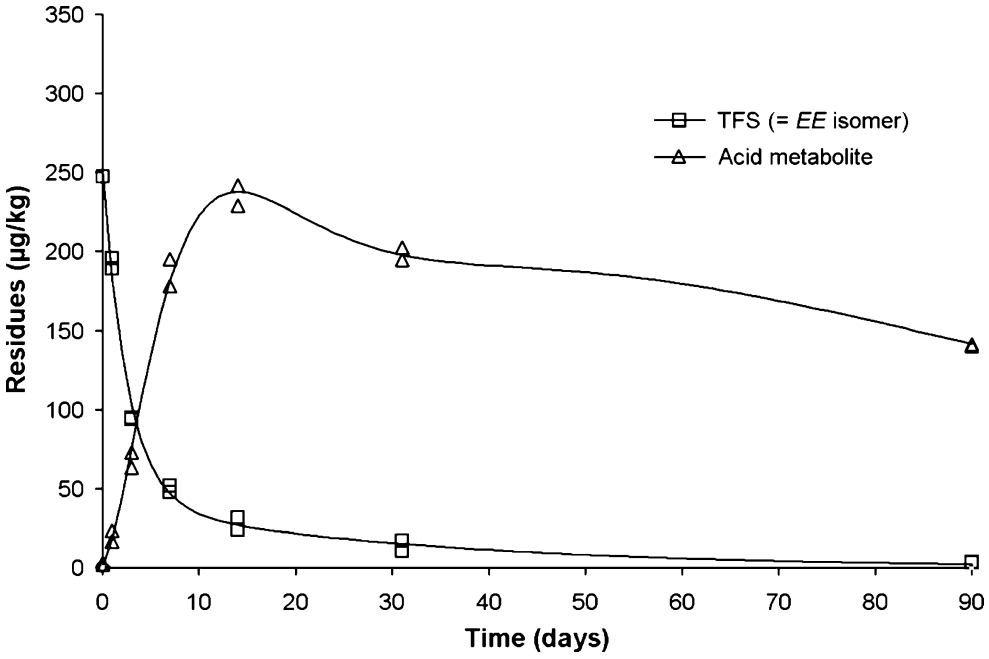

Fig. 2 Persistence of *EE*-TFS acid in Pune soil (India)

may take the route of *m/z* 395→192, and then *m/z* 148 is formed upon the elimination of CO_2. It is possible that the OCH_3 group in the *EZ*- and *ZZ*-acids interacts with the COOH group to form a ring structure, and CO_2 is lost during this process.

Anhydrous DMSO-D_6 was used as the solvent for NMR. All of the isomers could be identified in the pure form and no interconversion was observed. The chemical shifts relating to the 1-D and 2-D NMR measurements are presented in Tables 5 and 6, where the carbon numbers correspond to those in Fig. 1. The chemical shift data indicate that there is good baseline separation of the proton signal on C-10 for all four isomers; hence quantitative NMR is possible using this proton.

Monitoring acid metabolites of TFS in a soil environment

The *EE*-acid was identified as the major metabolite of TFS in soil. The concentration of the *EE*-acid in soil from Pune, India, increased over time, with the maximum accumulation recorded on the 14th day, after which it started to degrade to unidentified metabolites (Fig. 2). The rate of degradation of the *EE*-acid was slow, with a significant fraction of the peak concentration remaining on the 90th day (last sampling date). Hydrolysis was thus identified as the major route for the degradation of TFS in soil. The formation of the other isomers of TFS in soil—namely *EZ*, *ZE*, and *ZZ*—was negligible, which may be due to the absence of light during experimentation; hence, their acid metabolites were also not found in the test soil. Further research should be performed in sunlight to explore the build-up and rate of degradation of all four acid metabolites in soil.

Acknowledgements We thank the Ministry of Science and Technology, Government of India, for awarding a BOYSCAST fellowship to Kaushik Banerjee. We also thank Prof. Tsonko Kolev for helping us to interpret the IR and Raman spectra. Thanks are also due to Bayer Crop Science, Germany for providing us with reference substances, technical suggestions and literature support.

References

1. Ziegler H, Benet-Buchholz J, Etzel W, Gayer H (2003) Trifloxystrobin—a new strobilurin fungicide with outstanding biological activity. Pflanzenschutz-Nachr Bayer 56:213–230
2. Reuveni M (2000) Efficacy of trifloxystrobin (Flint), a new strobilurin fungicide, in controlling powdery mildews on apple, mango and nectarine, and rust on prune trees. Crop Prot 19(5):335–341
3. Ebeling M, Heimann KG, Schoefer S, Sonder K (2003) The human and environmental safety aspects of trifloxystrobin. Pflanzenschutz-Nachr Bayer 56:231–245
4. Banerjee K, Ligon AP, Spiteller M (2005) Photoisomerization kinetics of trifloxystrobin. Anal Bioanal Chem 382(7):1527–1533
5. Banerjee K, Ligon AP, Schürmann M, Preut H, Spiteller M (2004) Methyl-(*Z*,*Z*)-α-(methoxyimino)-2-[({1-[3-(trifluoromethyl)phenyl]ethylidene}amino)oxymethyl] benzeneacetate. Acta Crystallogr E60:525–526
6. Banerjee K, Ligon AP, Schürmann M, Preut H, Spiteller M (2004) Methyl-(*E*,*Z*)-α-(methoxyimino)-2-[({1-[3-(trifluoromethyl)phenyl]ethylidene}amino)oxymethyl] benzeneacetate. Acta Crystallogr E61:o1752–o1753
7. Banerjee K, Ligon AP, Schürmann M, Preut H, Spiteller M (2004) Methyl-(*Z*,*E*)-α-(methoxyimino)-2-[({1-[3-(trifluoromethyl)phenyl]ethylidene}amino)oxymethyl] benzeneacetate. Acta Crystallogr E61:o1569–o1570
8. Banerjee K, Ligon AP, Schürmann M, Preut H, Spiteller M (2005) Methyl-(*E*,*E*)-α-(methoxyimino)-2-[({1-[3-(trifluoromethyl)phenyl]ethylidene}amino)oxymethyl] benzeneacetic acid. Acta Crystallogr E61:o1528–o1529
9. Giradet M (1997) Activity of CGA 279202 and CGA 321113 on *Bortrytis cinerea* respiration (unpublished report No. 08G 97010 BO). Bayer CropScience AG, Monheim am Rhein, Germany
10. Reuveni M (2001) Activity of trifloxystrobin against powdery and downy mildew diseases of grapevines. Can J Plant Pathol 23(1):52–59
11. Banerjee K, Ligon AP, Spiteller M (2006) Environmental fate of trifloxystrobin in soils of different geographical origins and photolytic degradation in water. J Agric Food Chem 54 (25):9479–9487
12. EC (1995) Commission Directive 95/36/EC amending council directive 91/414/EEC concerning the placing of plant protection products on the market (Annexes I and II, Fate and behaviour in the environment). European Communities, Brussels
13. SETAC (1995) In: Lynch MR (ed) Procedures for assessing the environmental fate and ecotoxicity of pesticides. SETAC Europe, Brussels
14. BBA (1986) Guidelines for the official testing of plant protectants. Part IV, 4-1: Fate of plant protectants in soil—degradation, transformation and metabolism. BBA, Berlin
15. FDA (1987) Environmental assessment technical handbook. FDA, Washington, DC
16. Kaczor A, Szczepanski J, Vala M, Kozlowski H, Proniewicz L (2003) Infrared absorption spectra of 2-(hydroxyimino)propanohydroxamic and oxalodihydroxamic acids isolated in argon matrices. Phys Chem Chem Phys 5:2337–2343
17. Juchnovski IN, Kolev T, Binev JG (1981) Effects of neutral and anionic substituents on the carbonyl stretching band of substituted benzophenones. Spectrosc Lett 14(11 and 12):763–772
18. Wilson EB (1934) The normal modes and frequencies of vibration of the regular plane hexagon model of the benzene molecule. Phys Rev 45:706–714
19. Varsaniy G (1969) Vibrational spectra of benzene derivatives. Academic, New York, 1969
20. Varsaniy G (1974) Assignments for vibrational spectra of seven hundred benzene derivatives, vol. I and II. Adam Hilger, London
21. Roeges N (1994) A guide to complete interpretation of infrared spectra of organic molecules. Wiley-VCH, New York
22. Whiffen DH (1956) Vibrational frequencies and thermodynamic properties of fluoro-, chloro-, bromo-, and iodo-benzene. J Chem Soc 1350–1356
23. Kolev T, Nikolova B, Jordanov B, Juchnovski I (1985) Vibrational assignment of benzophenone and some of its isotopic species in the solid phase. J Mol Struct 129:1–10